J Mater Sci: Mater Med (2009) 20:2249–2257
DOI 10.1007/s10856-009-3804-3

Effect of Ca/P ratio and milling material on the mechanochemical preparation of hydroxyapaptite

Janeth Salas · Zully Benzo · Gema Gonzalez · Eunice Marcano · Clara Gómez

Received: 17 October 2007 / Accepted: 16 June 2009 / Published online: 11 July 2009

Abstract The mechanochemical transformation of $Ca(OH)_2$–$(NH_4)_2HPO_4$ with different Ca/P ratios 1; 1.5; 1.67 and 1.75 was carried out for different periods of time from 10 min to 24 h in a horizontal vibration mill using steel and agate vials and balls. The phase transformations obtained at each milling stage were characterized by X-ray diffraction, infrared spectroscopy and transmission electron microscopy. Complete transformation to hydroxyapatite took place during the first 5 h of milling, for Ca/P ratios 1.5 to 1.7, when milling was carried out with steel vials and balls. The contamination was not significant for the periods of milling studied for both milling media.

1 Introduction

Ceramic materials based on calcium phosphates such as hydroxyapatite (HAp) and β-tricalcium phosphates (β-TCP) have a wide range of potential applications for bone substitutes. These bioceramics favor bone reconstruction due to high properties of resorbability for β-TCP and good osteoconductivity for HAp. Hydroxyapatite is widely used in reconstructive orthopedic and dental surgery, both as massive filling of bone gaps and as a surface coating. In the latter case, it promotes adhesion between prostheses and bone [1].

Multiple techniques have been used for preparation of HAp powders by wet methods [2–13] and solid-state reactions [14–18]. Mechanochemistry is a solid-state synthesis method that takes advantage of the perturbation of surface-bonded species by pressure to enhance thermodynamic and kinetic reactions between solids [19]. Pressure can be applied at room temperature by different milling equipment ranging from low energy ball mills to high-energy stirred mills. The product obtained by the different authors depended on the method employed, the type of vial and the energy of the mill. Therefore, products with different morphology, stoichiometry, and level of crystallinity can be obtained by mechanochemical processes depending upon the technique and the milling materials used. The main advantages of this synthesis are simplicity and low cost. The chemical processes occurring during mechanical action on solids turned out to be more specific and versatile than they have been considered so far. This has stimulated the development of investigation in the field of mechanochemistry, a rapid developing area of chemical science. In the present work, the synthesis of calcium phosphate by mechanochemical transformation with different Ca/P ratios 1; 1.5; 1.67 and 1.75 has been carried out at different milling periods and the effect of using different milling materials such as agate and steel vials and balls in a horizontal vibrating mill has been studied.

2 Materials and methods

The solid reactants used were calcium hydroxide $Ca(OH)_2$, (96,7%, sigma Aldrich), ammonium biphosphate $(NH4)_2HPO_4$

J. Salas · Z. Benzo (✉) · E. Marcano · C. Gómez
Centro de Química, Instituto Venezolano de Investigaciones Científicas, IVIC, Apdo. Postal 21827, Caracas 1020, Venezuela
e-mail: zbenzo@ivic.ve

J. Salas
e-mail: jsalas@ivic.ve

G. Gonzalez
Laboratorio de Ciencia e Ingeniería de Materiales, Departamento de Ingeniería, Instituto Venezolano de Investigaciones Científicas, IVIC, Apto 21827, Caracas 1020, Venezuela
e-mail: gemagonz@ivic.ve

(99,99% sigma Aldrich). The mechanochemical transformation of $Ca(OH)_2$–$(NH4)_2HPO_4$ with different Ca/P ratios was carried out for different periods of time, from 10 min to 24 h in a horizontal vibration mill using steel and agate vials and balls. A Retsch vibratory Mill, Type MM-2 was used. FTIR spectra were obtained using a Nicolet 560 spectrometer. The process was monitored for each period by X-ray diffraction (XRD) and transmission electron microscopy (TEM). The X-ray diffraction was a Siemens D-500 difractometer with Cu-K_α radiation. The TEM observations were performed in a Phillips model CM12. Inductively Coupled Plasma optical emission spectroscopy (ICP-OES) was used for the determination of Ca and P in each product obtained using a Perkin Elmer spectrometer, model Optima 3000.

3 Results and discussion

The phase transformations obtained at each milling stage with each milling material used were characterized by X-ray diffraction, infrared spectroscopy and transmission electron microscopy analysis. The results are shown in Figs. 1–8. Table 1 shows the Ca/P ratio of the products, determined by ICP-OES, after the different milling periods with each milling material tool employed.

3.1 Grinding of reactants for the Ca/P ratio 1

Figure 1 shows the XRD pattern for this Ca/P ratio. It can be seen that the pattern varied with grinding time. The intensity of the peaks of the starting materials gradually decreased as a function of grinding time and the HAp phase begins to form as an incipient phase after grinding for 30 min. The XRD pattern also shows the formation of $NH_4CaPO_4{\cdot}H_2O$ from 5 h and remains present up to 24 h. Although, it is not expected the formation of HAp for a Ca/P molar ratio of 1, however, during milling a heterogeneous mixture is present and part of the reactants might reach a stoichiometric ratio corresponding to HAp. The initial reactants remain present up to 24 h, in steel as well as in agate vials. In general, the reactions taking place in both milling tools are very similar. The IR spectra (Fig. 2) for this mixture at the different milling periods show bands corresponding to phosphates and ammonium vibrations. The bands in the region 1100–1045, 963, 873, 604 and 562 cm^{-1} are attributed to phosphate vibrations. The bands at 1094, 1027 and 874 cm^{-1} could be attributed to the presence of HPO_4^{-2} groups, Koutsopoulos [20] attributes the 1027 cm^{-1} band to the presence of crystal imperfections and HPO_4^{-2} groups in nonstoichiometric HAp, the 1045 cm^{-1} vibration corresponds to the asymmetric P–O vibrating mode and the band at 963 cm^{-1} to the symmetric P–O vibrating mode. The bands at 604 and 562 cm^{-1} correspond to the U_4 bending mode of the O–P–O bonds. Also, the bands characteristic of ammonium U_4 (NH_4) group are seen in the regions 3300–2800 cm^{-1} and 1400–1500 [21]. In agate vials after 5 h of milling, a clear splitting of the U_4 (NH_4) modes is observed, this was attributed to lowering of the site symmetry of the ammonium ion [21]. For this period, the formation of $NH_4CaPO_4{\cdot}H_2O$ compound is observed. When steel vials were used the formation of this compound was observed after only 1 h. The band observed at 1650 cm^{-1} is probably adsorbed water [22, 23].

The FTIR results are in good agreement with the XRD patterns showing the presence of remaining starting material $(NH_4)_2HPO_4$, a new phase of calcium ammonium phosphate hydrate $NH_4CaPO_4{\cdot}H_2O$, and HAp, even after

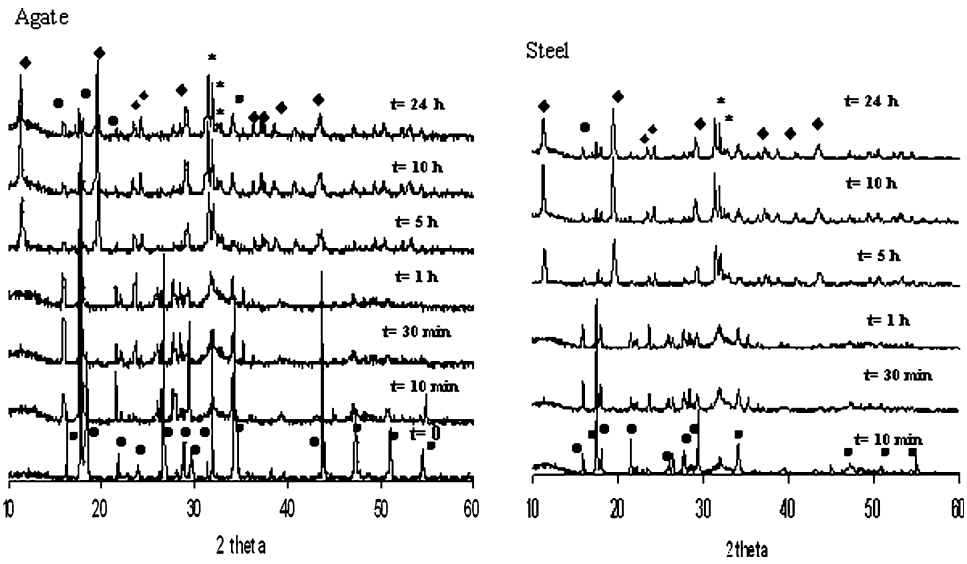

Fig. 1 XDR of Ca/P = 1 mixture milled during different periods. (*Asterisk*) HAp, (*filled square*) $Ca(OH)_2$, (*filled circle*) $(NH_4)_2{\cdot}HPO_4$, (*filled rhombus*) $CaNH_4PO_4{\cdot}H_2O$

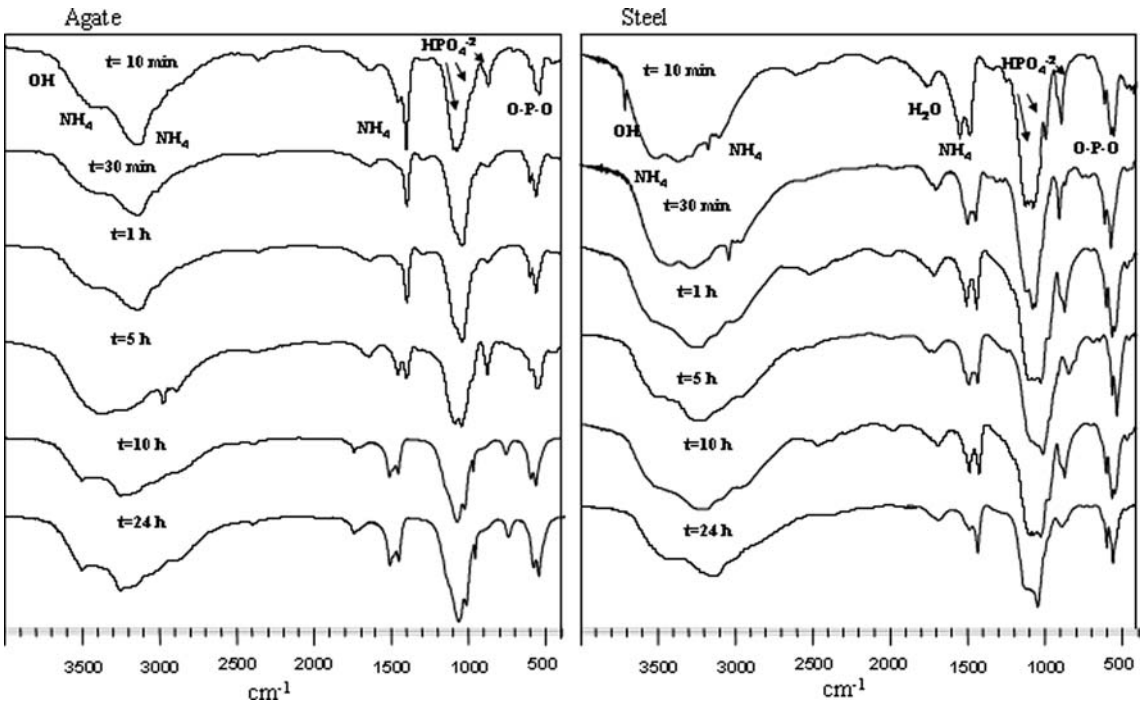

Fig. 2 FT-IR spectra of Ca/P = 1 mixture milled during different periods

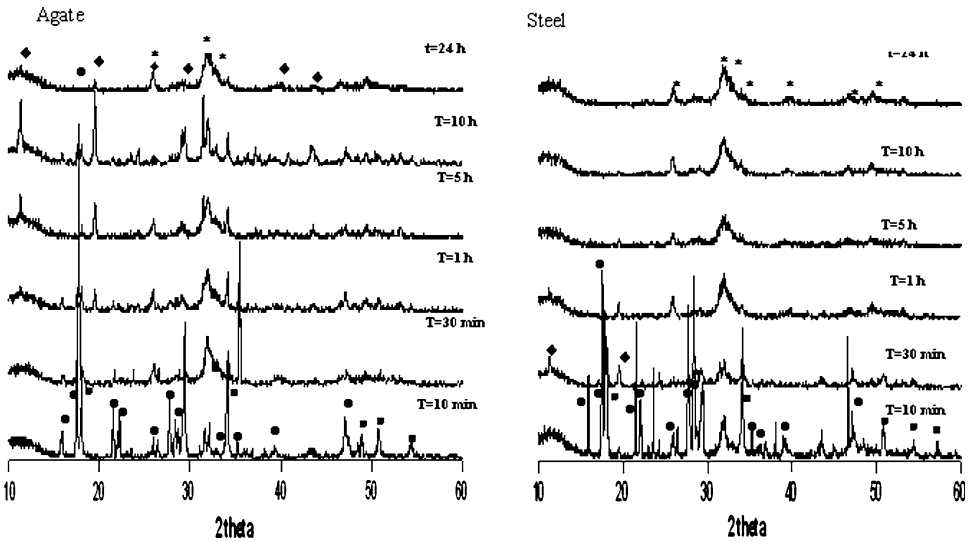

Fig. 3 XDR of Ca/P = 1.5 mixture milled during different periods. (*Asterisk*) HAp, (*filled square*) $Ca(OH)_2$, (*filled circle*) $(NH_4)_2{\cdot}HPO_4$, (*filled rhombus*) $CaNH_4PO_4{\cdot}H_2O$

milling for 24 h. Similar results were obtained in agate and steel vials.

3.2 Grinding of reactants in the Ca/P ratio 1.5

Figure 3 shows the XRD results for the Ca/P ratio 1.5 for the different milling periods.

Formation of Ca-deficient HAp was obtained after 24 h of milling in steel and in agate vials. It can be notice that the effect of grinding tools material on the phase transformations with milling time was more efficient in steel than in agate vials. HAp was formed from 1 h onwards in both milling media, however, when using steel after 5 h grinding time the reaction was complete and not remaining initial reactants were observed; however, when using agate vials even after 24 h milling time a small amount of the initial reactants and the $NH_4CaPO_4{\cdot}H_2O$ compound was still present. Therefore, steel milling tools are more efficient than agate tools to induce the phase transformations. Figure 4 shows the infrared spectra as a function of the grinding time. For agate tools from 30 min up to 24 h the vibration bands corresponding to NH_4 groups were present at 1456 and 1401 cm^{-1} and in the region 3300–2800 cm^{-1}. Also, the characteristic phosphate bands (1094, 1045, 963,

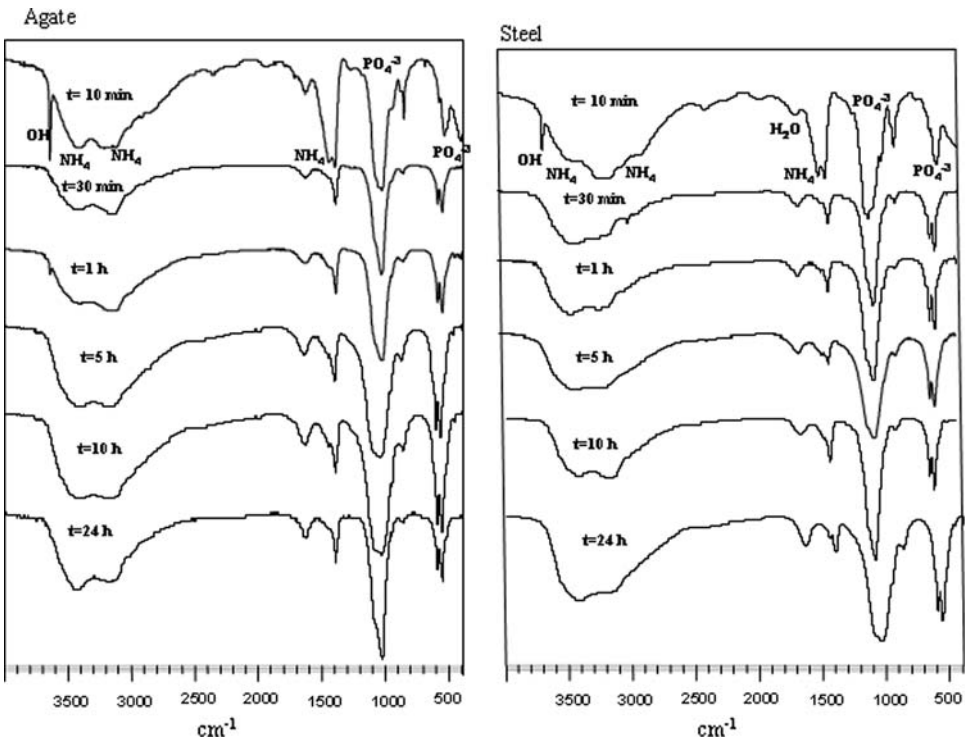

Fig. 4 FT-IR spectra of Ca/P = 1.5 mixture milled during different periods: **a** agate, **b** steel

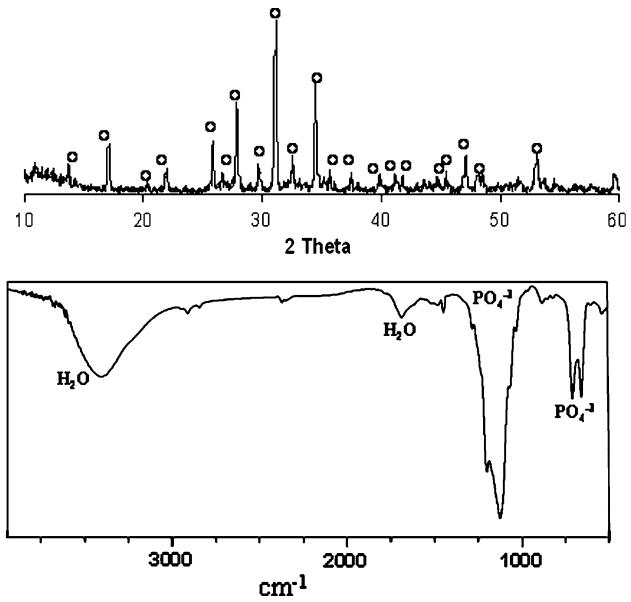

Fig. 5 DRX and FTIR of calcined samples at 800°C, Ca/P 1.5 milled in agate vials or steel vials

874, 604 and 562 cm^{-1}) were observed and the vibration bands of the hydroxyl groups at 3550 and 631 cm^{-1}. On the other hand, when milling was carried out in steel vials after 10 h the presence of $NH_4CaPO_4{\cdot}H_2O$ compound completely disappears and a calcium deficient HAp was the only phase observed by XRD and FTIR. In order to verify that calcium deficient HAp is effectively formed, the products obtained, after milling in both media for 24 h, were calcined at 800°C for 2 h as suggested by Ishikawa et al. [24] and Mostafa [25]. β-Tricalcium phosphate was formed after such thermal treatment, in agreement with the expected results (Fig. 5). The same result was obtained for both grinding materials.

3.3 Grinding of reactants in the Ca/P ratio 1.67

Figure 6 shows the XRD patterns for the different milling periods for Ca/P = 1.67, for both milling media. When milling was carried out in an agate vial, the compound $NH_4CaPO_4{\cdot}H_2O$ together with calcium deficient HAp was obtained and remained present up to 48 h of milling, indicating that the reaction in this milling material did not proceed completely. However, milling in steel resulted in formation of HAp, as the only product obtained. These differences in the products obtained using the different milling materials is attributed to the different impact energy generated by each material during the milling process.

The reaction is steel vials was completed after 5 h of milling by the total consumption of the initial reagents. The crystal size was 20 nm, measured from the XRD patterns applying the Scherrer equation:

$$d = \frac{K\lambda}{\beta \cos\theta}$$

where λ is the wavelength, β the width of peak at half maximum intensity, θ the diffraction angle, d the crystal size, and $K = 0.9$.

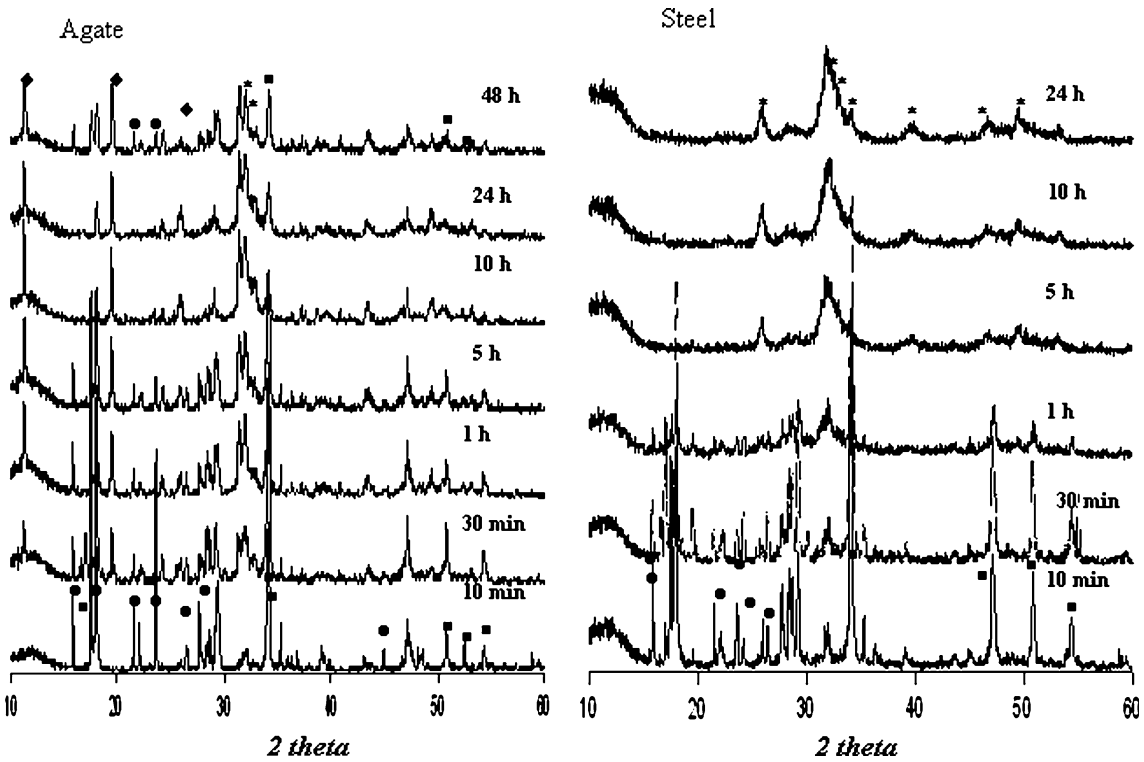

Fig. 6 XDR of Ca/P = 1.67 mixture milled during different periods. (*Asterisk*) HAp, (*filled square*) $Ca(OH)_2$, (*filled circle*) $(NH_4)_2{\cdot}HPO_4$, (*filled rhombus*) $CaNH_4PO_4{\cdot}H_2O$

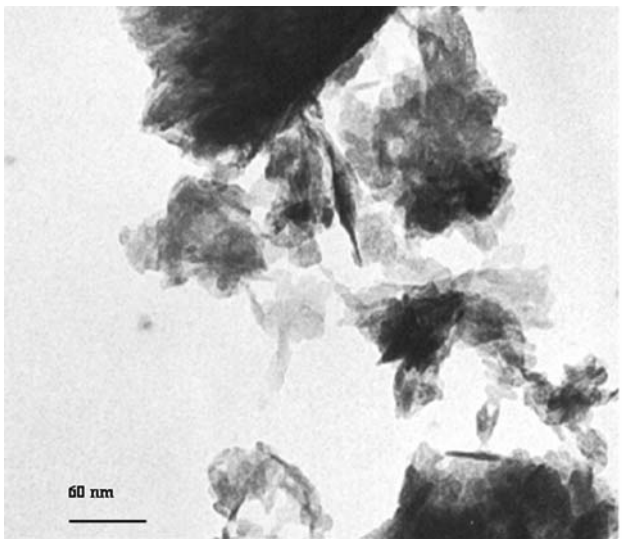

Fig. 7 Transmission electron microscopy bright field image of Ca/P = 1.67 mixture showing hydroxyapatite crystals formed after 5 h of milling

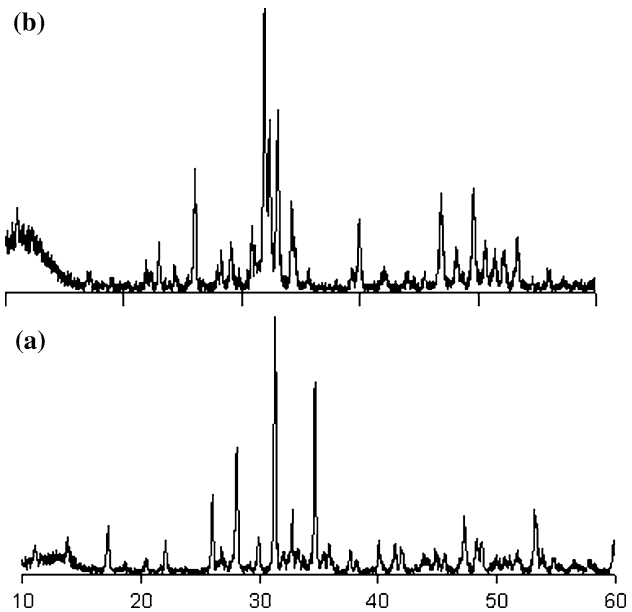

Fig. 8 DRX of calcined samples at 800°C, Ca/P = 1.67 milled in **a** agate vials showing the presence of β-tricalcium phosphate, **b** steel vials showing the presence of HAp

This result was in very good agreement with the observation by transmission electron microscopy (Fig. 7), which shows long narrow needle-shape and rounded crystals of average crystal size of 20 nm. Figure 8 shows the XRD of the calcined samples milled in steel and agate media, indicating that stoichiometric HAp was formed in steel milling media but calcium deficient HAp was obtained in agate vial, due to the presence of β-tricalcium phosphate after calcination.

Table 1 Ca/P ratios of products milled in steel or agate vials for different periods, determined by ICP

Time	Ca/P							
	1		1.5		1.67		1.75	
	Agate	Steel	Agate	Steel	Agate	Steel	Agate	Steel
10 min	1.01 ± 0.01	1.21 ± 0.07	1.58 ± 0.01	1.59 ± 0.05	1.69 ± 0.07	1.68 ± 0.01	1.77 ± 0.01	1.78 ± 0.01
30 min	1.19 ± 0.02	1.08 ± 0.02	1.52 ± 0.02	1.59 ± 0.02	1.69 ± 0.02	1.68 ± 0.02	1.73 ± 0.03	1.68 ± 0.01
1 h	1.27 ± 0.05	1.15 ± 0.04	1.54 ± 0.01	1.60 ± 0.04	1.68 ± 0.03	1.71 ± 0.04	1.79 ± 0.03	1.71 ± 0.01
5 h	1.15 ± 0.02	1.16 ± 0.08	1.56 ± 0.02	1.56 ± 0.02	1.68 ± 0.02	1.66 ± 0.01	1.81 ± 0.05	1.73 ± 0.01
10 h	1.13 ± 0.06	1.20 ± 0.08	1.59 ± 0.06	1.58 ± 0.03	1.67 ± 0.06	1.67 ± 0.08	1.79 ± 0.02	1.71 ± 0.01
24 h	1.25 ± 0.05	1.17 ± 0.09	1.59 ± 0.05	1.59 ± 0.04	1.67 ± 0.05	1.68 ± 0.09	1.85 ± 0.05	1.75 ± 0.01

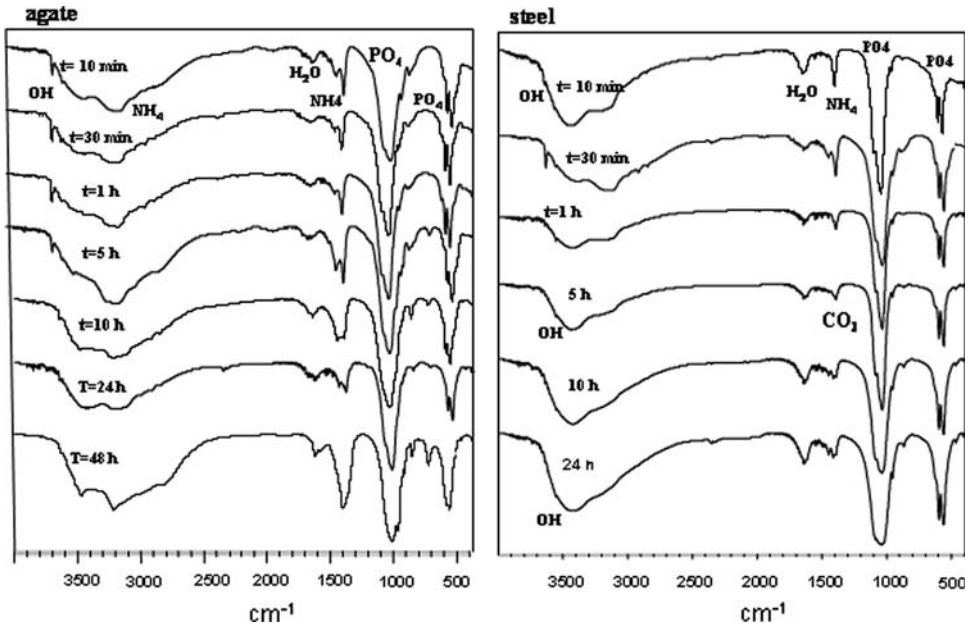

Fig. 9 FT-IR spectra of Ca/P = 1.67 mixture milled during different periods

The FTIR absorption spectra for these experiments (Fig. 9) showed some differences between the products obtained with both milling media, specially the presence of the NH_4 vibration bands in the regions, 3300–2800 cm^{-1} and 1400–1500 cm^{-1}, were observed in the products milled in agate vials up to 48 h, due to the presence of the initial reagents and the $NH_4CaPO_4{\cdot}H_2O$ compound, but not in the products milled in steel vials, after 1 h of milling. Also, a marked difference between both milling media was observed in the bands corresponding to the hydroxyl groups. The vibration band at 3570 cm^{-1} assigned to the hydroxyl group of HAp [20] was observed in the products milled in steel vials, from 1 h onwards. However, the OH vibration band at 3642 cm^{-1}, assigned to $Ca(OH)_2$, was observed in the products milled in agate vials, indicating that some remaining $Ca(OH)_2$ was still present, in agreement with the XRD results. The characteristic HAp bands (1094, 1045, 963, 631, 604 and 562 cm^{-1}) are observed in both milling media.

3.4 Grinding of reactants in the Ca/P ratio 1.75

For Ca/P = 1.75 (Figs. 10, 11) milling in agate materials showed the formation of HAp after 5 h. However, a small amount of $NH_4CaPO_4{\cdot}H_2O$ compound and remaining unreacted $Ca(OH)_2$ were present up to 24 h of milling. Milling in steels media showed the formation of HAp after only 1 h, and further milling resulted in total consumption of any remaining product, showing the presence of HAp as the only phase obtained after 5 h.

Therefore, the results obtained for the different Ca/P ratios using both milling materials clearly show that the milling materials nature strongly affect the final products obtained. For all Ca/P ratios studied milling in steel tools was more efficient than milling in agate, suggesting that the impact energy generated with steel tools is higher than the energy produced when using agate tools, resulting in higher energy transference to the compounds during the process and thus accelerating the kinetic of the phase

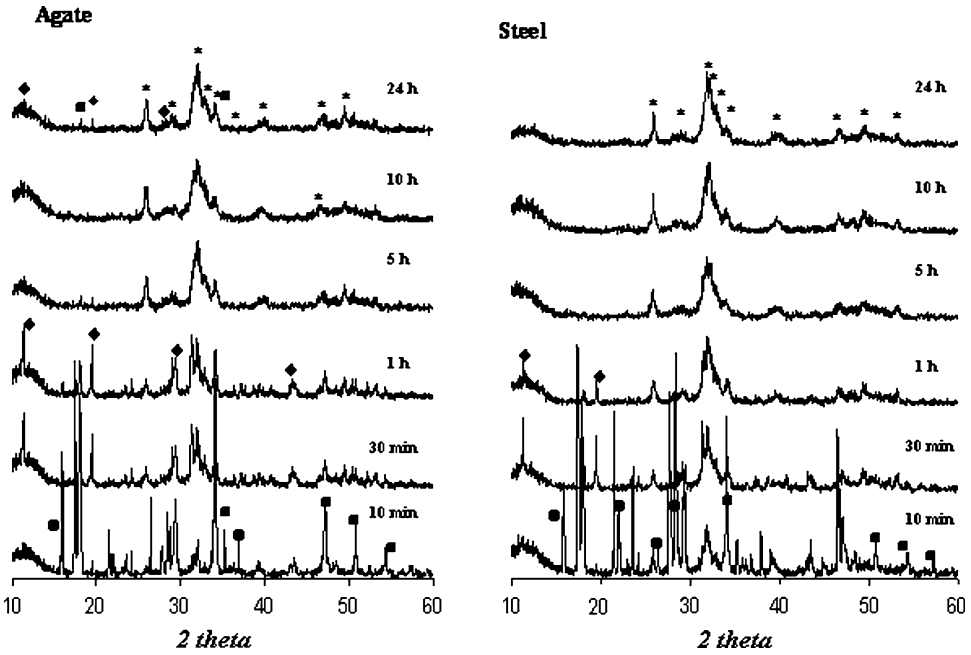

Fig. 10 XDR of Ca/P = 1.75 mixture milled during different periods. (*Asterisk*) HAp, (*filled square*) $Ca(OH)_2$, (*filled circle*) $(NH_4)_2{\cdot}HPO_4$, (*filled rhombus*) $CaNH_4PO_4{\cdot}H_2O$

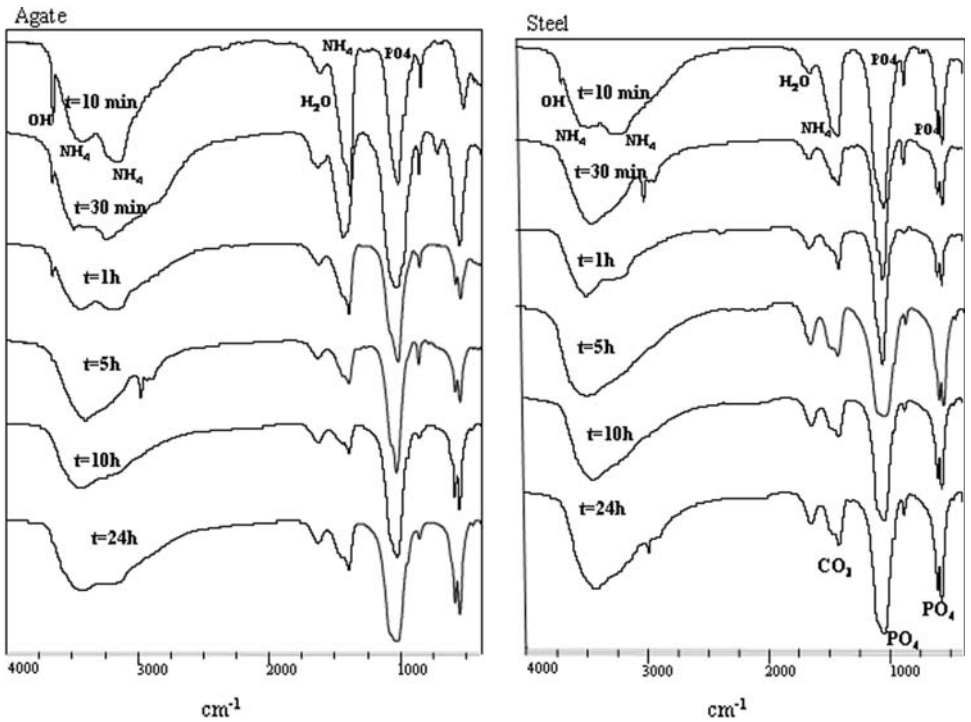

Fig. 11 FT-IR spectra of Ca/P = 1.75 mixture milled during different periods

transformations induced by milling. This could be attributed to the intrinsic physical properties of the milling materials employed, mainly to the elastic modulus that would have an effect on the impact energy produced during the milling process and therefore in the reactions taking place and in the final transformation of the reactants.

ICP measurements to detect the amount of possible contamination due to milling were carried out. The concentration of 14 elements analyzed was below the detection limit (50 μg/g). Tables 2 and 3 show the ICP results of the products milled in agate and steel vials, respectively, for the different milling periods.

Table 2 Chemical analysis determined by ICP, of products milled in agate vials for different periods

Tiempo	Hg	Mg	Fe	Cu	K	Cd	Ni	Cr	Co	Mn	As	Pb	Zn
10 min	≤80	≤50	≤50	≤100	≤50	≤50	≤50	≤50	≤50	≤50	≤80	≤50	≤50
30 min	≤80	≤50	≤50	≤100	≤50	≤50	≤50	≤50	≤50	≤50	≤80	≤50	≤50
1 h	≤80	≤50	≤50	≤100	≤50	≤50	≤50	≤50	≤50	≤50	≤80	≤50	≤50
5 h	≤80	≤50	≤50	≤100	≤50	≤50	≤50	≤50	≤50	≤50	≤80	≤50	≤50
10 h	≤80	≤50	≤50	≤100	≤50	≤50	≤50	≤50	≤50	≤50	≤80	≤50	≤50
24 h	≤80	≤50	≤50	≤100	≤50	≤50	≤50	≤50	≤50	≤50	≤80	≤50	≤50

Table 3 Chemical analysis determined by ICP, of products milled in steel vials for different periods

Tiempo	Hg	Mg	Fe	Cu	K	Cd	Ni	Cr	Co	Mn	As	Pb	Zn
10 min	≤80	≤50	≤50	≤100	≤50	≤50	≤50	≤50	≤50	≤50	≤80	≤50	≤50
30 min	≤80	≤50	≤50	≤100	≤50	≤50	≤50	≤50	≤50	≤50	≤80	≤50	≤50
1 h	≤80	≤50	≤50	≤100	≤50	≤50	≤50	≤50	≤50	≤50	≤80	≤50	≤50
5 h	≤80	≤50	≤50	≤100	≤50	≤50	≤50	≤50	≤50	≤50	≤80	≤50	≤50
10 h	≤80	≤50	≤50	≤100	≤50	≤50	≤50	≤50	≤50	≤50	≤80	≤50	≤50
24 h	≤80	≤50	≤50	≤100	≤50	≤50	≤50	≤50	≤50	≤50	≤80	≤50	≤50

4 Conclusions

The synthesis of nanometric hydroxyapatite was obtained after only 5 h of milling when steel vial were used for the Ca/P ratio of 1.67 and 1.75. For a Ca/P of 1.5 calcium deficient HA was obtained that transformed to β-tricalcium phosphates after heating at 800 °C.

This mechanochemical method, used to produce HAp, presents the advantage that the powder obtained is nanocrystalline with an average crystals size of 20 nm wide and 80 nm length. Formation of the products was more efficient when milling was carried out using steel tools.

Contamination of the products in any of the milling materials was below 50 ppb.

Acknowledgements The authors gratefully acknowledge the FONACIT projects No. LAB-1998003690 and G-2001000900 for financial support.

References

1. Sergo V, Sbaizero O, Clarke DR. Mechanical and chemical consequences of the residual stresses in plasma sprayed hydroxyapatite coatings. Biomaterials. 1997;18:477.
2. Silva CC, Pinheiro AG, Miranda MAR, Góes JC, Sombra ASB. Structural properties of hydroxyapatite obtained by mechanosynthesis. Solid State Sci. 2003;5:553.
3. Fernandez E, Gil F, Ginebra M, Driessens F, Planell J. Calcium phosphate bone cements for clinical applications. J Mater Sci: Mater Med. 1999;10:177.
4. Fanovich J, Porto J. Influence of temperature and additives on the microstructure and sintering behaviour of hydroxyapatites with different Ca/P ratios. J Mater Med. 1998;9:53.
5. Suchananek W, Yoshimura M. Processing and properties of hydroxyapatite-based biomaterials for use as hard tissue replacement implants. J Mater Res. 1998;13:94.
6. Yamashita K, Kanazawa T. Inorganic phosphate materials. Amsterdam, The Netherlands: Kodansha & Elsevier; 1989. p. 15.
7. Legeros RZ. Calcium phosphates in oral biology and medicine. Basel, Switzerland: Kager AG; 1991. p. 201.
8. Yoshimura M, Suda H. Hydroxyapatite and related compounds. Boca Raton, FL: CRC Press; 1994. p. 45.
9. Elliot JC. Structure and chemistry of the apatites and other calcium orthophosphates. Amsterdam, The Netherlands: Elsevier; 1994.
10. Suchanek W, Suda H, Yashima M, Kakihana M, Yoshimura M. Biocompatible whiskers with controlled morphology and stoichiometry. J Mater Res. 1995;10:521.
11. Liou S-C, Chen S-Y. Transformation mechanism of different chemically precipitated apatitic precursors into β-tricalcium phosphate upon calcinations. Biomaterials. 2002;23:4541.
12. Kim W, Zhang Q, Saito F. Mechanochemical synthesis of hydroxyapatite from $Ca(OH)_2$–P_2O_5 and CaO–$Ca(OH)_2$–P_2O_5 mixtures. J Mater Sci. 2000;35:5401.
13. Spadavecchia U, González G. Obtención de hidroxiapatita manométrica para aplicaciones médicas. Rev Fac Ing. 2007;22(4):37.
14. Kim W, Saito F. Mechanochemical síntesis of hydroxyapatite from constituent powder mixtures by dry grinding. J Chem Eng Jpn. 2000;35:768.
15. Yeong B, Junmin X, Wang J. Mechanochemical síntesis of hydroxyapatite from calcium oxide and brushite. J Am Ceram Soc. 2001;84:465.
16. Mochales C, El Briak-BenAbdeslam H, Ginebra MP, Terol A, Planell JA, Boudeville P. Dry mechanochemical synthesis of hydroxyapatites from DCPD and CaO: influence of instrumental parameters on the reaction kinetics. Biomaterials. 2004;25:1151.
17. Gonzalez G, Villalba R, Sargarzazu A. Synthesis of biomaterials by mechanochemical transformation. Mater Sci Forum. 2002;386–388:645.
18. González G, Sagarzazu A, Villalba R. Mechanochemical transformation of mixtures of $Ca(OH)_2$ and $(NH_4)_2$ HPO_4 or P_2O_5. Mater Res Bull. 2006;41(10):1902.

19. Gutman E. Mechanochemistry of materials. Cambridge, UK: Cambridge International Science; 1997.
20. Koutsopoulos S. Synthesis and characterization of hydroxyapatite crystal: a review study on the analytical methods. J Biomed Mater Res. 2002;62:600.
21. Cahil A, Soptrajanov B, Najdoski M, Lutz HD, Engelen B, Stefov V. Infrared and Raman spectra of magnesium ammonium phosphate hexahydrate (struvite) and its isomorphous analogues. Part VI: FT-IR spectra of isomorphously isolated species. NH_4^+ ions isolated in $MKPO_4{\cdot}6H_2O$ (M = Mg; Ni) and PO_4^{-3} ions isolated in $MgNH_4AsO_4{\cdot}6H_2O$. J Mol Struct. 2008;876:255.
22. LeGeros RZ. Biologically relevant calcium phosphates. In: Myers HM, editor. Calcium phosphates in oral biology and medicine. London: Basel; San Francisco: Karger; 1991. p. 4–45.
23. Farmer VC. The vibrations of protons in minerals: hydroxyl, water and ammonium. In: Farmer VC, editor. The Infrared spectra of minerals. London: Mineralogical Society; 1974. p. 137–182.
24. Ishikawas K, Ducheyne P, Radin S. Determination of the ratio in calcium-deficient hydroxyapatite using X-ray diffraction analysis. J Mater Sci: Mater Med. 1993;4:165.
25. Mostafa NY. Characterization, thermal stability and sintering of hydroxyapatite powders prepared by different routes. Mater Chem Phys. 2005;94:333.